Int. J. Chem. Sci.: 14(4), 2016, 2147-2156
ISSN 0972-768X
www.sadgurupublications.com

OVING HIGH TEMPERATURE CORROSION OF THE STEEL PIPE HIGH PRESSURE BOILER COATED BY TITANIUM CARBONITRIDE

W. APERADOR[a,*], J. BAUTISTA-RUIZ[b] and E. RUIZ[a]

[a]School of Engineering, Universidad Militar Nueva Granada, BOGOTÁ-COLOMBIA
[b]Universidad Francisco de Paula Santander, San José de Cúcuta, COLOMBIA

ABSTRACT

In this paper, the corrosion resistance of steel high pressure boiler steel pipe (ASTM A335) is studied coated and uncoated of Carbo-Titanium Nitride (TiCN), grown on substrates 316 steels using co-sputtering r.f. The coatings were studied by potentiodynamic polarization curves Tafel using corrosive salts (vanadium pentoxide V_2 O_5 and Na_2 SO_4 sodium sulfate). The layers of Ti-C-N were grown varying the nitrogen flow to study its influence on the high temperature properties of these coatings, in addition to the bias voltage variation. Through of the technique of X-ray diffraction, it was found formation titanium carbonitride phases with orientation (200) and (111) and ESD spectroscopy shows an increase in the content of C and Ti with increasing nitrogen flow decreasing for high flows with -50V Bias. It found a decrease in the corrosion rate for the three coatings, additionally it decreases with increasing atomic nitrogen content.

Key words: Carbo-titanium nitride, Corrosion, Bias.

INTRODUCTION

Ternary coatings as TiCN, which are widely used for their mechanical properties (high hardness) can increase the life of cutting tools. In the search for materials besides high hardness, they also exhibit low coefficient of friction, high resistance to the corrosion and good electrical optical properties. It found that can combine properties of different materials to produce a single coating with superior properties to metal nitrides[1,2]. With nanocomposites, it has reached above 50 GPa hardness with grain size of the nanoparticles of the order of 10 nm coated with an amorphous phase of only a few atomic monolayers[3,4]. For these size crystals forming networks of dislocations is inhibited and thus the main mechanism of deformation is slipping plastic grain within the amorphous matrix[5]. The titanium Carbo

*Author for correspondence; E-mail: g.ing.materiales@gmail.com

Nitride (TiCN) is an inorganic compound formed by the interaction between ions of titanium, carbon and nitrogen, which form covalent bonds, ionic type requiring dissociation energy high link contributing to its high hardness[6,7]. The carbon and nitrogen causes an increase of the hardness of a material compared with the material block. When deposited on steels as thin film causes an increase in the surface hardness of steel.

Titanium is a transition element such as zirconium, vanadium, chromium, niobium, molybdenum, among others, which presents structure electronic an incomplete d layer[8]. Such electronic structure allows titanium to form substitutional solid solutions with many elements such as carbon and nitrogen, with a factor of size up to 20%[9]. Titanium has been listed as a light metal, although its density. TiN and TiC are similar materials having high hardness, good wear resistance with a high melting point and good chemical resistance[10]. Also they considered industrially important materials and have many applications in cutting tools and machine parts, especially as coatings[11].

TiCN coatings have not emerged as an important enough PVD coating. It is due to difficulties in processing, control of stoichiometry, the residual stress and the choice of suitable hydrocarbon carrier gas, which sometimes is methane and other acetylene[12]. The high temperature corrosion commonly occurs in boilers and furnaces in most cases by the combustion of coal causing a chemical process, where most steels have its metal surface in combustion ashes whose composition consists of mixtures of sulphates and chlorides, generating problems such as decrease in heat transfer, which leads to corrosion in an accelerated manner[13,14]. This is because most low carbon alloys, have restriction because after the 650°C corrosion occurs at high temperatures causing a decrease in mechanical properties. The chromium alloyed steels and nickel provide good performance over 1200°C, due to its austenitic type structure, however after subjecting them to close to 700°C temperatures in prolonged periods, it is presented to oxidative attack causing corrosion[15].

In this investigation coatings were obtained by mixing carbon, nitrogen and titanium grown by rf sputtering technique deposited on ASTM A335 steel substrates. As variables, it is handled the bias voltage applied to the substrate between 0 and -50V. Subsequently the structural properties shall be characterized by X-ray diffraction and scanning electron microscopy, the corrosion properties at high temperatures was performed in an oven which was adapted to a potentiostat.

EXPERIMENTAL

The electrochemical cell consists of an array of 3 electrodes: the working electrode, the reference electrode and auxiliary electrode. The working electrode was welded to a

platinum wire, which served as an electrical conductor, this wire was also placed inside a ceramic tube of mullite industrial grade so only the specimen was exposed to the corrosive environment. The reference electrode and counter electrode were built with high purity platinum wire, which were introduced into a mullite tube resistant to high temperatures; the hollow parts between the specimen and the ceramic tube were sealed with refractory cement as the spaces of the other electrodes.

The corrosive agent used in the test is composed of a mixture of pentoxide vanadium V_2O_5 and sodium sulfate Na_2SO_4 analytic grade to concentrations (percentage of weigh) 50:50, the mixture were macerated during 45 minutes in mortar for homogenize, then these were placed in a porcelain crucible of 30 g that was inserted inside on a vertical furnace. The electrochemical cell was placed in the furnace and the heating starts from room temperature to 700°C needed to perform the electrochemical tests (Fig. 1). The internal temperature was monitored by mean of a type k thermocouple connected to a temperature controller. To resemble a boiler environment was determined the use of a mixture of oxidizing gas $99\%O_2$-$1\%SO_2$.

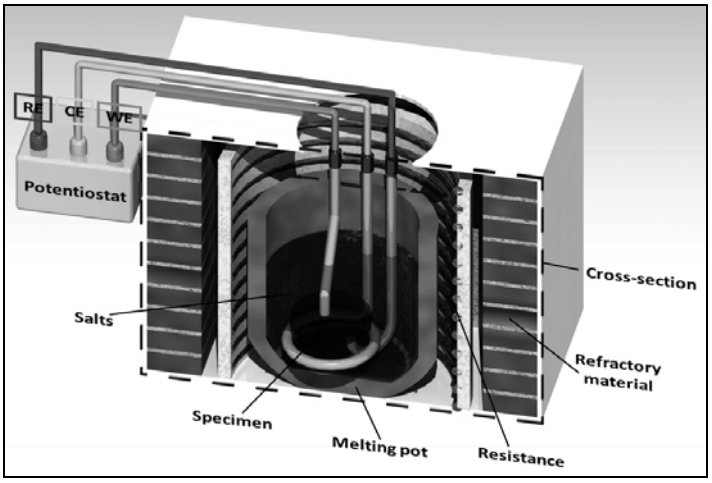

Fig. 1: Oven used for the electrochemical tests at high temperatures

In order to obtain the polarization curve a potential difference of ± 200 mV was applied at a scan speed of 1 mV/s in potentiodynamic form, rate and potential corrosion were obtained through Tafel extrapolation using a Gamry Instruments potentiostat. The potential corrosion values (Ecorr) and the corrosion current density (icorr) is determined through the extrapolation Tafel method using the software GamryEchem Analyst. The anodic and cathodic polarization curves were obtained after 3 hours of exposure to corrosive medium, time in which the corrosion potential stabilized.

The XRD measurements were perform in Bragg Brentano traditional configuration on Empyream diffractometer with a 240 mm incident beam radio, the focal line of the copper tube present $K_{\alpha 1}$ 1.540598 Å and $K_{\alpha 2}$ 1.544426 Å radiation. The generator settings were 45kV and 40 mA, 20-90° 2θ range, step size 0.0400° and a step time of 2 s. In the incident beam a nickel attenuator was used, 1° divergent slit, 2° anti-scatter slit and a 0.04 rad soller grid. In the diffracted beam a 0.25° receiving slit, a 0.50° anti-scatter slit and 0.04 rad soller grid was used. The interpretation of the results was developed in High Score software with ICSD PANanalytical database and the free version COD.

RESULTS AND DISCUSSION

Energy dispersive X-ray spectroscopy

In Fig. 2, the nitrogen content in each of the coatings with respect to the variation of Bias Potential indicated it generates income metal nitrides this reaction is very important because due to their income generated in the crystal structure in each case an increase in properties such as high hardness, corrosion resistance, biocompatibility and thermal stability[16-19]. So the income of an appreciable amount, cause greater protection against corrosion phenomena at high temperatures, titanium carbo nitrides system are compounds in which the nitrogen atom occupies the interstices of compact closed structures of metals.

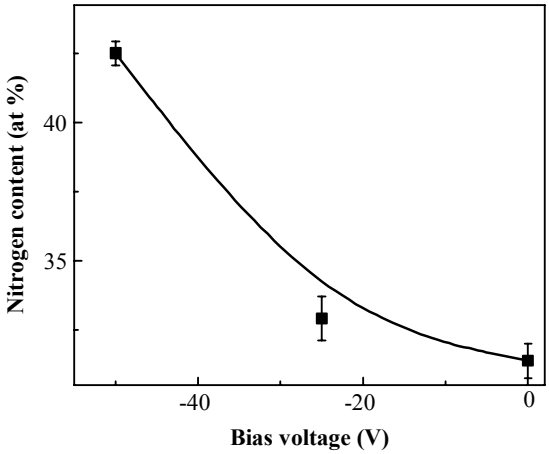

Fig. 2: Nitrogen content of each of the coatings obtained after Bias voltage variation, the assay was generated by EDS probe

The analysis by Energy Dispersive X-ray Spectroscopy (EDS) shows that the coatings are hyper-stoichiometric nature since the properties as in this case the chemical stability at high temperatures varies with the composition interstitial nitrides achieve

maximum stability when they reach their stoichiometry, as in the case of -25V and -50V Bias[20]. This is generated due to carbide titanium-nitrogen bond found in these compounds. The nitrogen atom is a very small element, therefore, the interstitial nitrides are formed very easily, metal carbides possess host structures, which are interstitial forming nitrides[21-23].

X-ray Diffraction

Fig. 3 shows the diffraction patterns in X-ray corresponding to grazing angle TiCN layers was observed, thus, a clear progression of intensity in the (111) plane at 2θ = 34.55°, by increasing the bias voltage increased intensity because a greater number of crystallites that are oriented in said preferential direction is generated also can be seen that this preferred orientation (111). It is present in all three systems tested the pattern corresponding to 0V bias diffraction, indicates a preferred orientation corresponding to the peak (220) the link formed by the metal and carbon[24-26].

In the diffraction pattern of the layer with a voltage of -50V, some contributions associated with the reflections of the bonds formed by carbon, nitrogen and titanium are observed, but with greater intensity regarding exhibit by the system without potential Bias, it is possible to observe that the experimental pattern for the different intensities in relation to 0V and -25V systems this is due to the mismatch attributed network due to tensile stress and compression presented by the layers as a result of deposition parameters specifically the negative bias voltage applied to the substrate (bias voltage)[27].

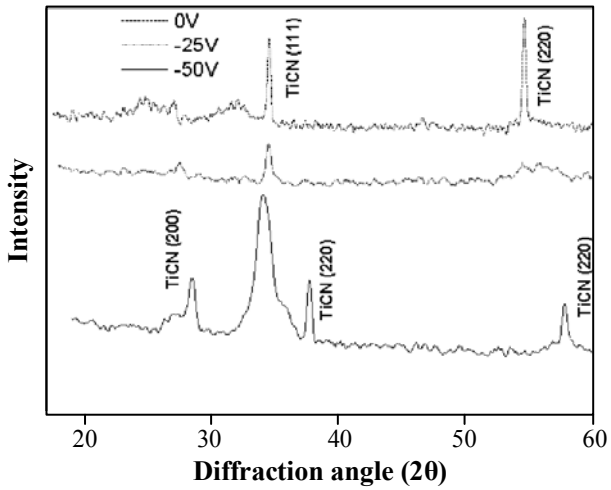

Fig. 3: XRD for different coatings for different crystal structures depending on the voltage of Bias

Polarization curves Tafel

In Fig. 4, the polarization curves where the three coatings are analyzed at a constant temperature of 700°C are analyzed increasing negative potential Bias. It generates a significant improvement against the corrosion rate as is the decrease. This is because at 0 V bias increased diffusion is generated, produce a greater thickness of the oxidized, bring about layer by isothermal oxidation, a suitable characteristic of the evaluated coatings is their performance against the change in volume due to increased temperature wherein a volumetric expansion, which is caused by various reasons including corrosion and the increased temperature. Because ionic bonds and covalent into coatings behavior resembles a ceramic material so they generally do not support a change in volume are formed. In this case, the coatings are not at high increased protection against corrosion and improvement of mechanical properties of ceramic materials.

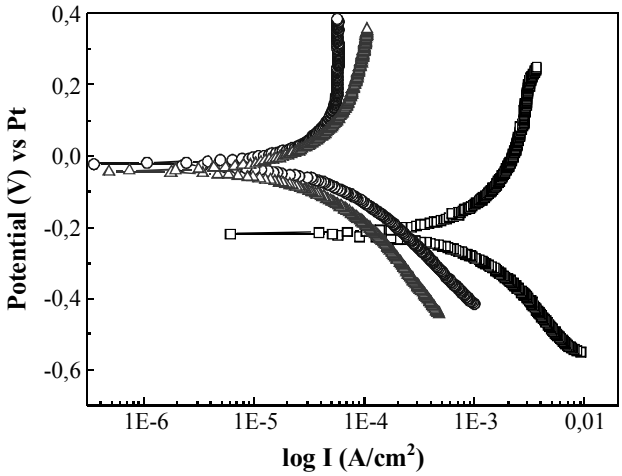

Fig. 4: Polarization curves assessed at high temperatures using corrosive salts as vanadium pentoxide and sodium sulfate

Regarding the study of the fracture of the coating, it was found that occurs when the material during operation undergoes transformation of crystal structure when subjected to temperature changes in a medium such as corrosive salts. In materials such as titanium carbide it has been identified that this phase transformation occurs at higher rates in the interfaces where metal oxidation reaction develops therefore nitrogen has been added in the coating in order to minimize the oxidation reaction to other materials selected according to the application of the material and because the bias voltage by reducing the entry of nitrogen in the coating is greater an increase in protection is generated[28]. Thermodynamically, the TiCN coatings behave differently due to the crystal structures found in all three systems

tested; therefore the compound that helps stabilize the crystal structure is to - 50V as observed in XRD.

In Fig. 4, Tafel polarization curves are observed the potential created buffer zones to 700°C, corrosion potentials projection cathode areas are related to coatings and Bias -25 and -50 V, the difference is 200 mV with respect system that has no voltage Bias[29]. The polarization curve of TiCN presents a general dissolution in the anode zone, since there is an increased oxidation and subsequent potential to 220 mV in the anode zone. There is a small increase in the area generating a density increase corrosion Bias samples with potential generate a stabilizing region generating a constant potential degradation. This corrosion resistance at high temperatures creates a layer whose stability is not adequate as it gradually increasing current density is observed. The importance of this region is that it behaves as a diffusion barrier of reaction products treated as a general dissolution[30].

In Table 1, we obtained, the values of current density and corrosion rate, it is evident that the system has less protection corresponds to the system that has no variation of bias potential, generating a high current value this corroborates corrosion in the polarization curves, where the curve has the largest displacement to the right, which implies an increased flow of dissolution and therefore in the corrosion rate, since they are directly proportional[31]. Mixtures with potential -25Vand -50V, presented the lower value of corrosion rate, which means that are more resistant to corrosion in the presence of Na_2SO_4 and V_2O_5. Regarding these mixtures, it is observed that increased sulfur diffusion alloy/oxide interface is yield generating fracture in the coating, because of the difference in thermal expansion coefficients between the substrate and the oxide layer.

Table 1: Parameters corrosion potential, corrosion current density and corrosion rate of the three systems evaluate, the potential Bias difference applied is observed and its electrochemical response

	0 V	**-25 V**	**-50 V**
Potential (V) vs Pt	-0.21	-0.044	-0.020
Current density (A/cm^2)	1.18×10^{-3}	3.26×10^{-5}	2.59×10^{-5}
Corrosionrate (μmy)	4.76×10^{-5}	1.28×10^{-6}	1.09×10^{-6}

CONCLUSION

In this study, the corrosion behavior of hot-Titanium Carbo Nitride was observed deposited by the technique of reactive sputtering evaluated in contact corrosive salts and

using Tafel polarization curves, the values obtained using this technique allow to find a behavior for each of the coatings, generally is obtained that the corrosion potential is higher for specimens that have Bias and current density and corrosion rate decreases due to application of potential Bias no a difference between -25V and -50V, since the decrease of these parameters versus 0 V is similar. Structural change was examined generating coatings and determined that the change in the corrosive properties it is due to the nitrogen content in the composite mixture.

ACKNOWLEDGEMENT

We thank the financial support from the Universidad Militar Nueva Granada, contract number ING- 2100-2016.

REFERENCES

1. K. Wang, H. Y. Jiang, Y. X. Wang, Q. D. Wang, B. Ye and W. J. Ding, Mater. Des., **95**, 545 (2016).
2. K. A. Kuptsov, Ph. V. Kiryukhantsev-Korneev, A. N. Sheveyko and D. V. Shtansky, Surf. Coat. Technol., **216**, 273 (2013).
3. V. Sáenz de Viteri, M. G. Barandika, U. Ruiz de Gopegui, R. Bayón, C. Zubizarreta, X. Fernández, A. Igartua and F. Agullo-Rueda, J. Inorg. Biochem, **117**, 359 (2012).
4. R. J. Talib, A. M. Zaharah, M. A. Selamat, A. A. Mahaidin and M. F. Fazira, Procedia Eng., **68**, 716 (2013).
5. P. Alvaredo, S. A. Tsipas and E. Gordo, Int. J. Refract. Met. Hard. Mater., **36**, 283 (2013).
6. A. A. Matei, I. Pencea, M. Branzei, D. E. Trancă, G. Ţepeş, C. E. Sfăt, E. Ciovica (Coman), A. I. Gherghilescu and G. A. Stanciu, Appl. Surf. Sci., **358**, 572 (2015).
7. M. Roca-Ayats, G. García, M. Soler-Vicedo, E. Pastor, M. J. Lázaro and M. V. Martínez-Huerta, Int. J. Hydrogen Energy, **40**, 14519 (2015).
8. R. Chen, J. P. Tu, D. G. Liu, Y. J. Mai and C. D. Gu, Surf. Coat. Technol., **205**, 5228 (2011).
9. Y. H. Cheng, T. Browne, B. Heckerman and E. I. Meletis, Surf. Coat. Technol., **205**, 4024 (2011).
10. R. A. Antunes, A. C. D. Rodas, N. B. Lima, O. Z. Higa and I. Costa, Surf. Coat. Technol., **205**, 2074 (2010).

11. D. G. Liu, Y. J. Pan, W. Q. Bai and J. P. Tu, Surf. Coat. Technol., **266**, 88 (2015).

12. N. Madaoui, N. Saoula, B. Zaid, D. Saidi and A. Si Ahmed, Appl. Surf. Sci., **312**, 134 (2014).

13. P. Alvaredo, C. Abajo, S. A. Tsipas and E. Gordo, J. Alloys Compd., 591, 72 (2014).

14. K. Balázsi, I. E. Lukács, S. Gurbán, M. Menyhárd, L. Bacáková, M. Vandrovcová and C. Balázsi, J. Eur. Ceram. Soc., **33**, 2217 (2013).

15. P. Alvaredo, D. Mari and E. Gordo, Int. J. Refract. Met. Hard. Mater., **41**, 115 (2013).

16. A. Engström, J. Mouzon, J. M. Córdoba, R. Tegman and M-L. Antti, Mater. Lett., **81**, 148 (2012).

17. J. C. Sánchez-López, M. D. Abad, I. Carvalho, R. Escobar Galindo, N. Benito, S. Ribeiro, M. Henriques, A. Cavaleiro and S. Carvalho, Surf. Coat. Technol., **206**, 219 (2012).

18. L. Escobar-Alarcon, V. Medina, Enrique Camps, S. Romero, M. Fernandez and D. Solis-Casados, Appl. Surf. Sci., **257**, 9033 (2011).

19. Y. Abe, K. Mori, F. Hatashita, T. Shiba, W. Daodon and K. Osakada, J. Mater. Process. Technol., **234**, 195 (2016).

20. K. Dejun, W. Jinchun, G. Haoyuan and W. Wenchang, Rare Met. Mater. Eng., **44**, 3000 (2015).

21. Y. Sun, C. Lu, H. Yu, A. K. Tieu, L. Su, Yue Zhao, H. Zhu and C. Kong, Mater. Sci. Eng., A, **625**, 56 (2015).

22. H. Li, Q. Wang, M. Zhuang and J. Wu, Vacuum, **112**, 66 (2015).

23. A. Tang, S. Liu and F. Pan, Prog. Nat. Sci., **23**, 501 (2013).

24. Y. Peng, H. Miao and Z. Peng, Int. J. Refract. Met. Hard. Mater., **39**, 78 (2013).

25. L. Shan, Y. Wang, J. Li, H. Li, X. Wu and J. Chen, Surf. Coat. Technol., **226**, 40 (2013).

26. W. Tillmann and S. Momeni, J. Phys. Chem. Solids, **90**, 45 (2016).

27. Y. Yang, N. Guo and J. Li, Surf. Coat. Technol., **219**, 1 (2013).

28. J. Zheng, J. Hao, X. Liu, Q. Gong and W. Liu, Surf. Coat. Technol., **209**, 110 (2012).

29. Z. Y. Zeng, H. Q Xiao, X. H Jie and Y. M Zhang, Trans. Nonferrous Met. Soc. China, **25**, 3716 (2015).

30. Q. Wang, F. Zhou, K. Chen, M. Wang and T. Qian, Thin Solid Films, **519**, 4830 (2011).

31. Q. Wang, F. Zhou, X. Wang, K. Chen, M. Wang, T. Qian and Y. Li, Appl. Surf. Sci., **257**, 7813 (2011).

Revised : 21.07.2016 *Accepted : 23.07.2016*